Available online at www.sciencedirect.com
ScienceDirect
Trans. Nonferrous Met. Soc. China 23(2013) 2011−2020
Transactions of Nonferrous Metals Society of China
www.tnmsc.cn

Preparation and oxidation behaviour of electrodeposited Ni−CeO_2 nanocomposite coatings

Hai-jun ZHANG, Yue-bo ZHOU, Jian-Feng SUN

College of Materials Science and Engineering, Heilongjiang Institute of Science and Technology, Harbin 150027, China

Received 15 June 2012; accepted 19 November 2012

Abstract: Ni−CeO_2 nanocomposite coatings with different CeO_2 contents were prepared by codeposition of Ni and CeO_2 nanoparticles with an average particle size of 7 nm onto pure Ni surfaces from a nickel sulfate. The CeO_2 nanoparticles were dispersed in the electrodeposited nanocrystalline Ni grains (with a size range of 10−30 nm). The isothermal oxidation behaviours of Ni−CeO_2 nanocomposite coatings with two different CeO_2 particles contents and the electrodeposited pure Ni coating were comparatively investigated in order to elucidate the effect of CeO_2 at different temperatures and also CeO_2 contents on the oxidation behaviour of Ni−CeO_2 nanocomposite coatings. The results show that the as-codeposited Ni−CeO_2 nanocomposite coatings have a superior oxidation resistance compared with the electrodeposited pure Ni coating at 800 °C due to the codeposited CeO_2 nanoparticles blocking the outward diffusion of nickel along the grain boundaries. However, the effects of CeO_2 particles on the oxidation resistance significantly decrease at 1050 °C and 1150 °C due to the outward-volume diffusion of nickel controlling the oxidation growth mechanism, and the content of CeO_2 has little influence on the oxidation.
Key words: codeposition; nanocomposite coating; oxidation; reactive-element effect

1 Introduction

The composite electrodeposition technique is a low-cost and low-temperature method suitable for producing metal matrix composite coatings with excellent properties for diverse purposes such as wear and abrasion resistance [1−3]. In this process, fine particles or whiskers are suspended in the electrolyte and embedded in the growing metal layer. Recently, rare earth oxide particles have been also used in electrodeposition process of composite due to their excellent wear and corrosion resistance and potential application in surface protection [4−7] rather than oxidation resistance. PENG et al [8−10] reported that the electrodeposited Ni−La_2O_3 composites show improved oxidation resistance compared with electrodeposited Ni films because the rapid outward diffusion of Ni along the grain-boundary was inhibited by the second-phase La_2O_3 nanoparticles and also by segregated La^{3+} ions from the dissolution of La_2O_3 nanoparticles which originally existed in the composite coatings. This phenomenon is referred to as "reactive-element effect (REE)", which was first reported in 1937 [11]. Various theories have been put forward to explain the effect [12−14], but there still is dispute. CeO_2 is another important reactive-element oxide, which is added into alloys by different techniques, such as alloying and sol−gel deposition to enhance the high temperature oxidation performance of Ni [15−17]. SEN et al [18] reported that the codeposition of CeO_2 nanoparticles improved the corrosion resistance of Ni film in 3.5% NaCl solution due to the inert CeO_2 particles acting as a physical barrier to the initiation and development of pitting corrosion. The formation of many micro-corrosion cells due to the presence of nano-sized CeO_2 in the Ni−CeO_2 nanocomposite and the longer circuitous path to reach the substrate in the Ni−CeO_2 nanocomposite compared with nanocrystalline pure Ni may also contribute to the improved corrosion resistance of Ni. QU et al [19] and XU et al [20] also reported that the codeposition of CeO_2 nanoparticles significantly improved the oxidation resistance of Ni film, but the microstructural characteristics of scale are limited in an attempt to elucidate further the effect of CeO_2 on the

Foundation item: Project (11531319) supported by Scientific Research Fund of Heilongjiang Provincial Education Department, China
Corresponding author: Yue-bo ZHOU; Tel: +86-451-88036159: E-mail: zhouyuebo760309@163.com, ybzhou@imr.ac.cn
DOI: 10.1016/S1003-6326(13)62690-4

oxidation of Ni. In the present work, the isothermal oxidation behaviours of Ni−CeO_2 nanocomposite coatings with two different CeO_2 contents and electrodeposited pure Ni coating were comparatively investigated in air at 800, 1050 and 1150 °C. Microstructural characteristics were analyzed in detail and related to the observed behaviour in an attempt to elucidate further the role of rare earths in the oxidation of metals.

2 Experimental

Samples with dimensions of 15 mm×10 mm×2 mm were cut from an electrolytic nickel plate. They were ground to a final 800# SiC paper. After ultrasonically cleaning in acetone, they were electrodeposited (on all sides) with a 40 μm-thick film of Ni−CeO_2 from a nickel sulfate bath with the addition of a certain content of CeO_2 nanoparticles (commercial product: cerium (IV) oxide from NanoScale Materials, Inc., Manhattan, KS with the purity >99% and the mean particle size of 7 nm). The current density used was 3 A/dm^2, the bath temperature was 35 °C, and the pH is 5.6−6.2. The detailed coating process has been provided in Ref. [21]. For comparison, a 65 μm-thick Ni film was also electroplated on the Ni using the same electrolytic bath and the same parameters as those used for Ni−CeO_2 nanocomposite coatings but without adding CeO_2 nanoparticles.

The surface morphologies of the prepared coatings were examined by a Camscan MX2600FE type scanning electron microscope/energy dispersive X-ray spectroscope (SEM/EDS) to determine the composition of the Ni−CeO_2 nanocomposite coatings. The mass fraction of ceria was determined by using the mole ratio of cerium to oxygen of 1: 2 determined by the chemical formula CeO_2. The isothermal oxidation experiments were carried out in air at 800 °C for 30 h, 1050 °C and 1150 °C for 20 h, respectively. The mass measurements were conducted after fixed time intervals using a balance with 0.01 mg sensitivity. Three parallel samples were adopted for acquring average mass change during the thermal exposure. By X-ray diffraction (XRD), SEM/EDS and transmission electron microscopy (TEM), characterization of coatings before and after oxidation was conducted. Electroless Ni-plating was plated on the surface of the oxidized specimens to prevent the spallation of the scales for observing cross-sections.

3 Results

3.1 Microstructure

Figure 1 shows the relationship between the content of codeposited CeO_2 nanoparticles and the concentration of CeO_2 nanoparticles in the bath. It is seen that the mass fraction of the codeposited CeO_2 nanoparticles in the composite coatings strongly depended on the content of nanoparticles in the plating bath, which is in agreement with Ref. [4]. The highest content of codeposited CeO_2 particles is achieved at CeO_2 concentration of 100 g/L. The curve is quite similar to the well-known Langmuir adsorption isotherms supporting a mechanism based on an adsorption effect. The codeposition of CeO_2 by the electrodeposition technique may be attributed to the adsorption of CeO_2 nanoparticles on the cathode surface, as suggested by Guglielmi's two-step adsorption model [22]. Once the particle is adsorbed, metal begins building around the cathode slowly, encapsulating and incorporating the particles. The highest concentration of CeO_2 nanoparticles on the composite is due to saturation in adsorption on the cathode surface.

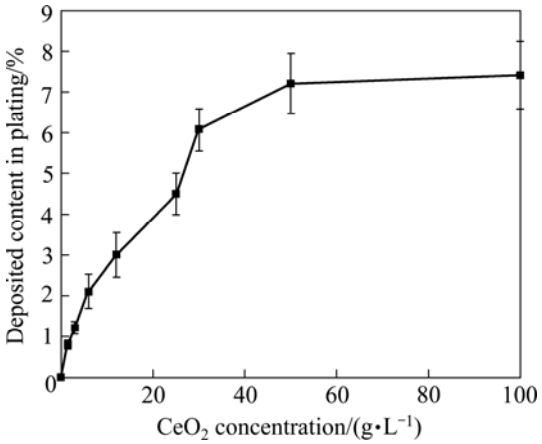

Fig. 1 Effect of CeO_2 concentration in bath on content of CeO_2 nanoparticles in composite coating

SEM surface morphologies of the electrodeposited pure Ni coating and the Ni−CeO_2 nanocomposite coatings containing different contents of CeO_2 nanoparticles are shown in Fig. 2. The electrodeposited Ni coating shows a regular pyramidal structure due to a typical Ni growth texture [23], as seen in Fig. 3(a). However, with the addition of CeO_2 nanoparticles, the grain size is reduced and the morphology is changed to spherical structure, as seen in Figs. 2(b)−(d). The change in the morphology can be associated to the change from preferred orientation for Ni film to random orientation for Ni−CeO_2 nanocomposite coatings, as seen from the XRD pattern in Fig. 3(b). Furthermore, the grain size of Ni crystalline decreased with the increase of codeposited CeO_2 particles content, which could significantly influence the properties of the composite coatings. It is evident that CeO_2 nanoparticles are uniformly distributed in the Ni matrix at a lower CeO_2 particles content. However, at a higher CeO_2 particles content of about 4.5%, the CeO_2 nanoparticles tend to form agglomerates,

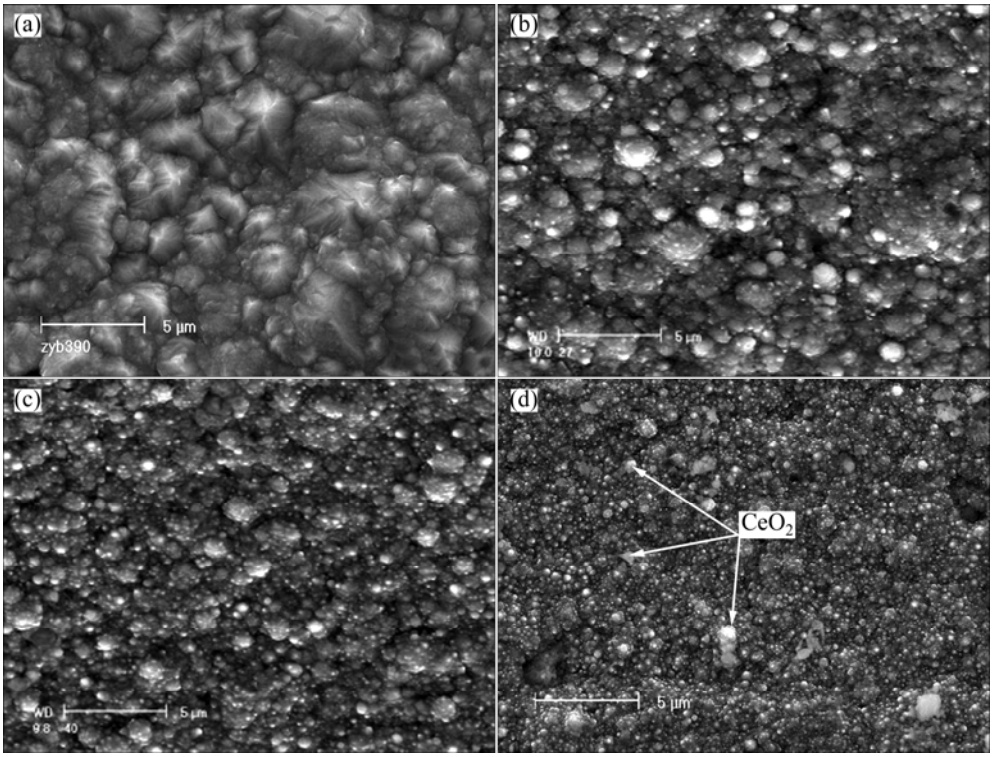

Fig. 2 SEM images of as-deposited pure Ni and Ni−CeO_2 nanocomposite coatings containing different contents of CeO_2 nanoparticles: (a) Pure Ni; (b) 0.8% CeO_2; (c) 3.0% CeO_2; (d) 4.5% CeO_2

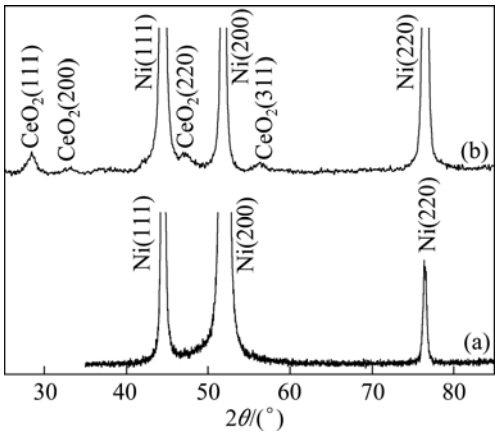

Fig. 3 XRD patterns of as-deposited pure Ni-film (a) and Ni−7.2%CeO_2 nanocomposite coating (b)

as seen in Fig. 2(d), which would significantly decrease the oxidation resistance of Ni−CeO_2 nanocomposite coatings [20] and be helpless to elucidate the effect of CeO_2 on the oxidation of Ni−CeO_2 nanocomposite coatings. Thus, two Ni−CeO_2 nanocomposite coatings with lower CeO_2 particles contents of about 0.8% and 3.0% were chosen for oxidation experiment in this work. TEM investigation [21] reveals that the Ni grains in Ni−CeO_2 composite coatings were in nano scale, with a size in the range of 10−30 nm according to the measurement from a few hundred grains selected randomly, which are smaller than the Ni grains in the electrodeposited pure Ni film in a size range of 15−60 nm [24]. Both films formed numerous twins. No defects such as pores and cracks were seen. The CeO_2 peaks corresponding to (111), (200), (220) and (311) are observed along with the nickel peaks in Fig. 3(b), which further confirmed the presence of CeO_2 particles in the Ni−CeO_2 nanocomposite coatings.

3.2 Oxidation resistance

The isothermal oxidation kinetic curves of the as-deposited pure Ni film and Ni−CeO_2 nanocomposite coatings at 800 °C for 30 h, 1050 °C and 1150 °C for 20 h are illustrated in Figs. 4(a), (b) and (c), respectively, which show that the codeposited CeO_2 nanoparticles significantly improved the oxidation resistance of the as-deposited pure Ni coating. All coatings obeyed the parabolic rate law to a good approximation in the whole duration of the test. The calculated parabolic rate constants for oxidation of various coatings at different temperatures are listed in Table 1. From Fig. 4 and Table 1, it could be found that there was no much difference between the mass gains of Ni−CeO_2 nanocomposite coatings with different CeO_2 contents, especially at 1050 °C and 1150 °C, implying that the CeO_2 particles content has little influence on the oxidation of Ni−CeO_2 nanocomposite coatings at temperature above 1000 °C. In another words, the content of the CeO_2 nanoparticles in the nickel film may be not a crucial factor affecting

the film oxidation. At the same time, the effect of CeO_2 on decreasing the scaling rate decreased with the increasing oxidation temperature.

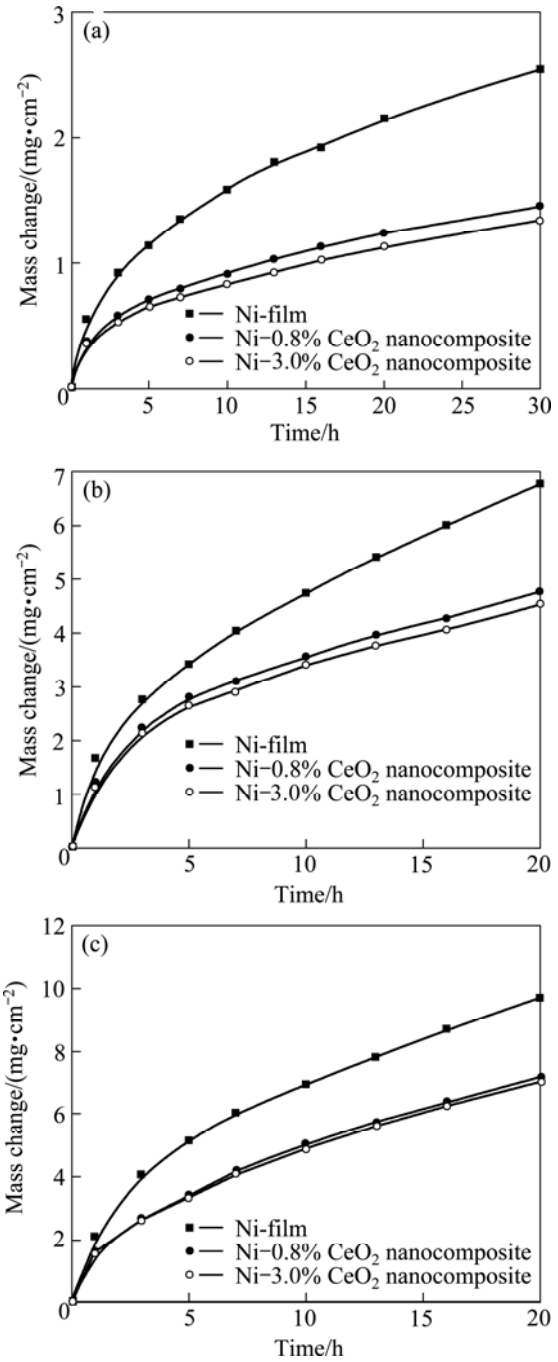

Fig. 4 Kinetic curves of isothermal oxidation in air at 800 °C (a), 1050 °C (b) and 1150 °C (c)

Table 1 Calculated oxidation parabolic rate constants

Temperatures/°C	Rate constant/(10^{-10}g^2·cm^{-4}·s^{-1})		
	Ni-film	Ni−0.8%CeO_2	Ni−3.0% CeO_2
800	0.59	0.195	0.166
1050	6.41	3.16	2.85
1150	13.08	7.13	6.83

XRD results show that the scales formed on the various coatings consist of NiO after oxidation at different temperatures. To clarify the difference in the oxidation performance of various coatings, surface and cross-sectional morphologies of the scales formed were investigated.

Faceted NiO grains formed on the various coatings after 30 h oxidation at 800 °C, as presented in Fig. 5. However, NiO grains formed on the as-deposited pure Ni film are about 7.5 μm, which are larger than the NiO grains formed on Ni−0.8% CeO_2 and Ni−3.0% CeO_2 nanocomposite coating with mean size less than 2.5 μm and 2.0 μm at the scale/gas interface, respectively, as seen in Figs. 5(c) and (e). From the corresponding cross-section in Fig. 5(b), the scales formed on the as-deposited pure Ni film showed a duplex structure, with the outer layer consisting of the coarse columnar crystals and the inner layer consisting of fine equiaxed grains. Large voids were observed in the inner layer or at the scale/ metal interface. The total scale thickness for the as-deposited pure Ni film is about 26 μm, and the thickness ratio of inner layer to outer layer is 0.5, as seen in Fig. 5(b). NiO scale formed on both Ni−CeO_2 nanocomposite coatings also exhibited a porous structure with smaller voids in the inner layer and the total thickness is about 12 μm for Ni−0.8% CeO_2 coating and 10 μm for Ni−3.0% CeO_2 nanocomposite coating, as seen in Figs. 5(d) and (f). EDS results show that the outer layer is pure NiO; however, Ce-rich bright oxides, as arrowed in Figs. 5(d) and (f), existed in the inner NiO layer. From Fig. 5(f), it could be found that some NiO nodules penetrated into Ni−CeO_2 nanocomposite coatings. Examination of fracture cross-sections indicated that the scale formed on Ni−3.0% CeO_2 nanocomposite coating also exhibited a similar duplex structure, as seen in Fig. 6. However, the thickness ratio of inner layer to outer layer is about 1, higher than that in the as-deposited pure Ni film.

Similar surface and cross-sectional morphologies of the NiO scales also existed on the various coatings after 20 h oxidation at 1050 °C and 1150 °C, as seen in Figs. 7 and 8, respectively. However, surface NiO grains were large compared with those formed at 800 °C. Smaller NiO grains size could be also observed on the surface of Ni−CeO_2 nanocomposite coatings with higher CeO_2 content. The corresponding cross-sections of the scales clearly exhibited a thin scale of NiO with Ce-rich bright oxides dispersing in the inner layer formed on Ni−CeO_2 nanocomposite coatings (Figs. 7(d), (f), Figs. 8(d) and (f)), while a thicker NiO scale with a porous inner layer grew on the electrodeposited pure Ni coating, as seen in Fig. 7(a) and Fig. 8(a). Examination of fracture cross-sections indicated that only a relatively coarse-grained, columnar layer formed on the electrodeposited pure Ni

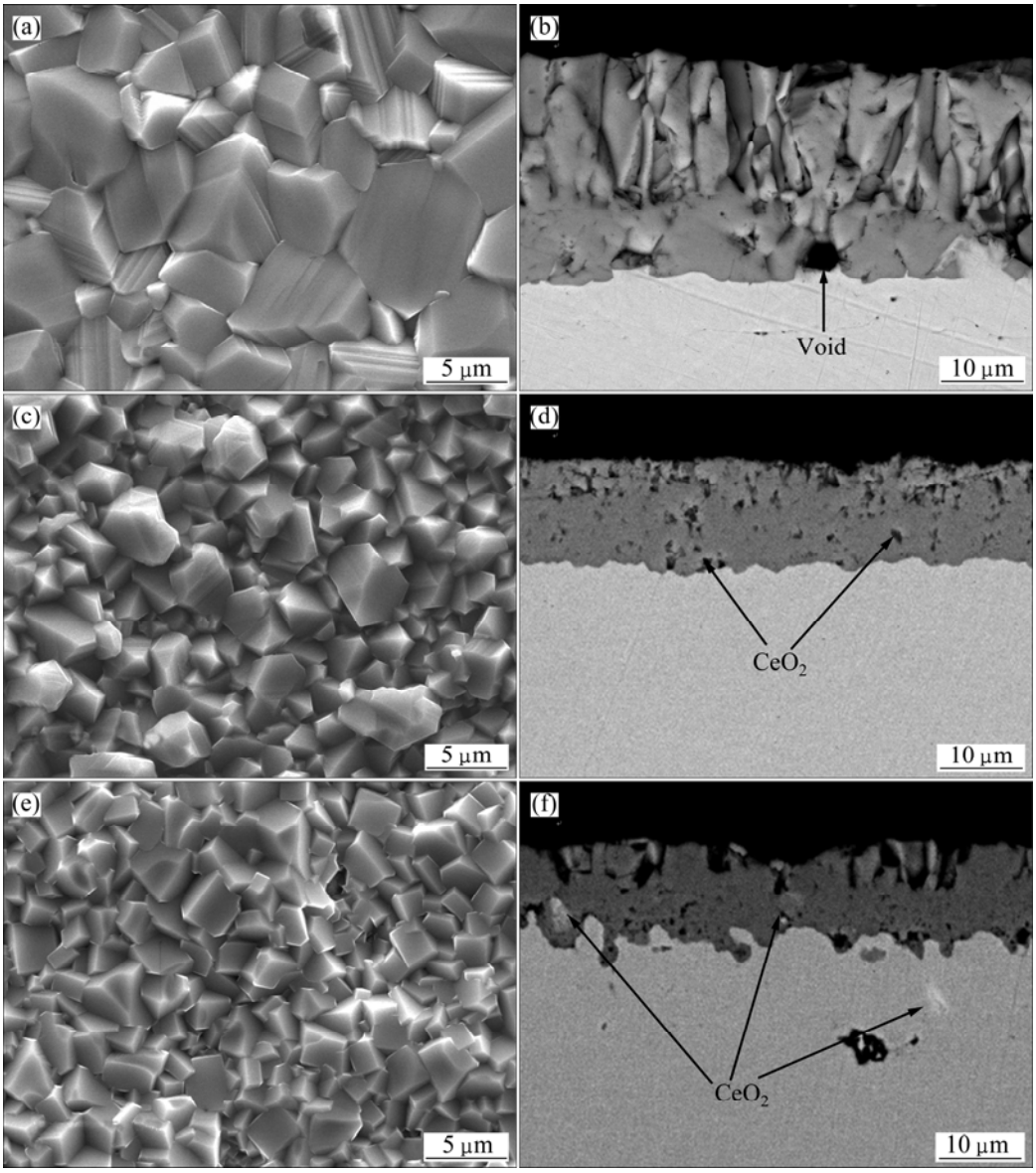

Fig. 5 Surface (a, c, e) and cross-sectional (b, d, f) morphologies of NiO scales formed on various samples after isothermal oxidation in air at 800 °C for 30 h: (a), (b) Ni-film; (c), (d) Ni−0.8% CeO_2 nanocomposite coating; (e), (f) Ni−3.0% CeO_2 nanocomposite coating

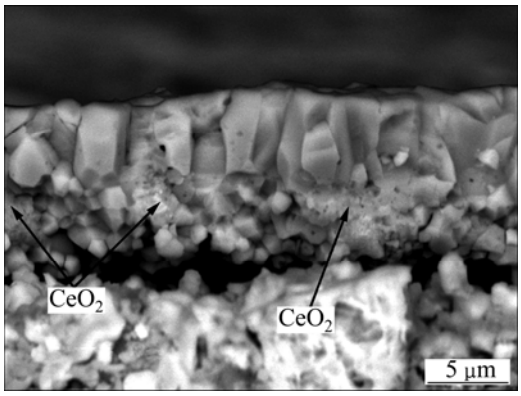

Fig. 6 Fracture section of scale formed on Ni−3.0% CeO_2 nanocomposite coating after isothermal oxidation in air at 800 °C for 30 h

coating after oxidation at 1050 °C for 20 h, while the scale formed on Ni−3.0% CeO_2 nanocomposite coating was still duplex with a similar inner and outer layer thickness, as seen from Fig. 9.

4 Discussion

Much evidence [15−17, 25−28] supports the growth of a double-layer scale on nickel at temperatures lower than 1000 °C: a more compact and coarse columnar outer layer due to the outward diffusion of nickel along grain boundaries, and a porous and fine equiaxed grain inner layer due to the inward diffusion of oxygen to the scale/metal interface through discontinuous "short-circuit" paths, such as voids, microchannels, and

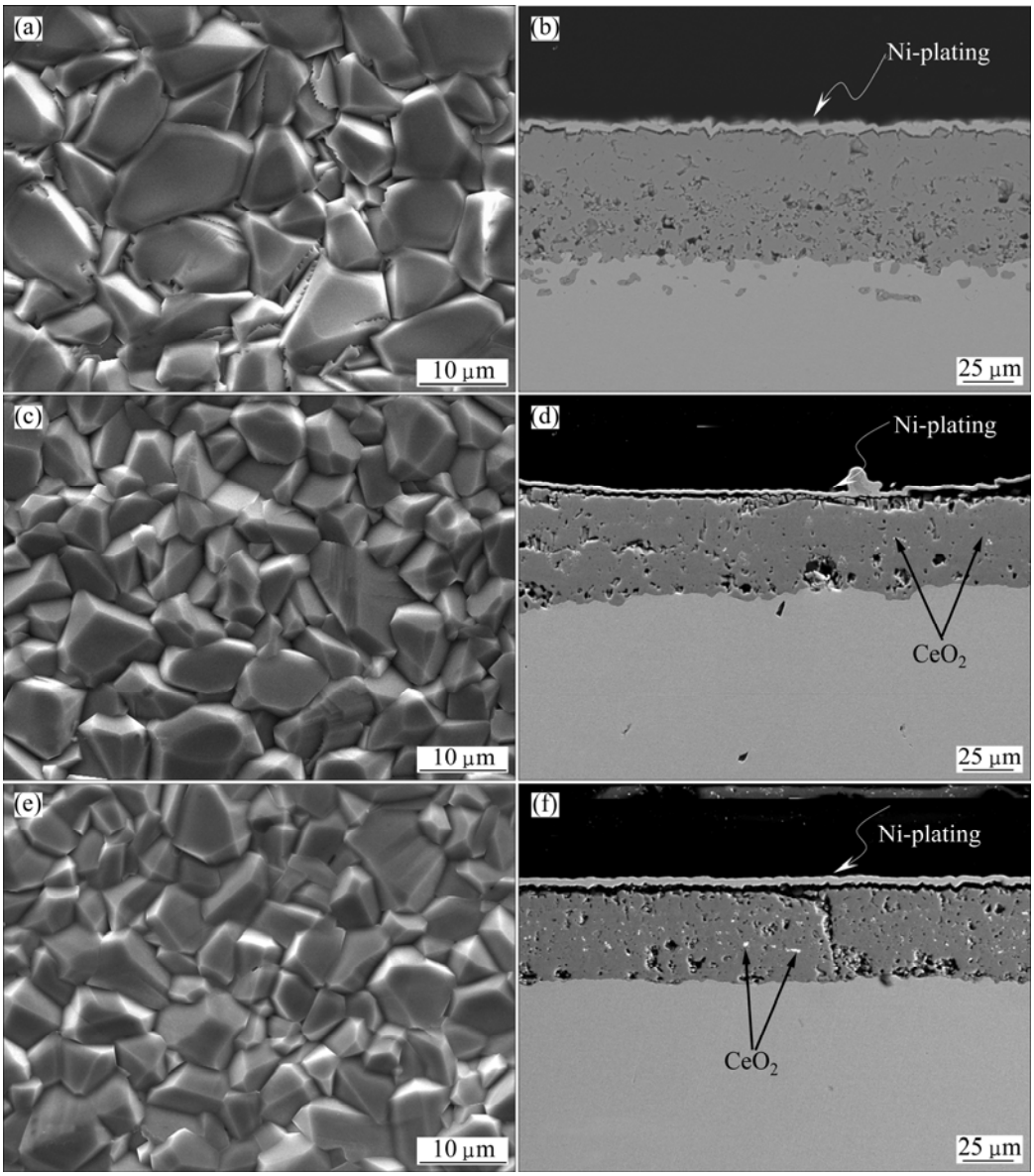

Fig. 7 Surface (a, c, e) and cross-sectional (b, d, f) morphologies of NiO scale formed on various samples after isothermal oxidation in air at 1050 °C for 20 h: (a), (b) Ni-film; (c), (d) Ni−0.8% CeO_2 nanocomposite coating; (e), (f) Ni−3.0% CeO_2 nanocomposite coating

fissures in the outer oxide scale. At this temperature, the outward diffusion of nickel is predominantly over inward oxygen diffusion, and a thicker columnar outer layer occurs with the increasing temperature. At temperatures above 1000 °C, faceted grains and simplex scale consisting of a coarse columnar crystal are usually observed due to the outward-volume diffusion of nickel through NiO scales and the minimization of surface energy.

According to this experimental results, the formation of duplex scale at 800 °C or simplex scale at 1050 °C and 1150 °C suggested that a similar oxidation mechanism occurred for the electrodeposited nickel coating, which would be affected by the defect formed on coating surface such as dislocation or twin acting as fast "short-circuits" diffusion paths and thereby the oxidation of Ni film was accelerated [8−10]. Similar to electrodeposited pure Ni coating, defects, such as twins and dislocation, are also created in the Ni−CeO_2 nanocomposite coatings. TEM image showed that the grain sizes of Ni grains in Ni−CeO_2 nanocomposite coatings were finer than those in the electrodeposited pure Ni coating. Based purely on microstructure, it seems certain that the growth rate of NiO on the Ni−CeO_2 nanocomposite coatings should be at least as fast as that on the electrodeposited pure Ni coating. Moreover, the NiO scale grown on the Ni−CeO_2 nanocomposite coatings was fine, and should grow even

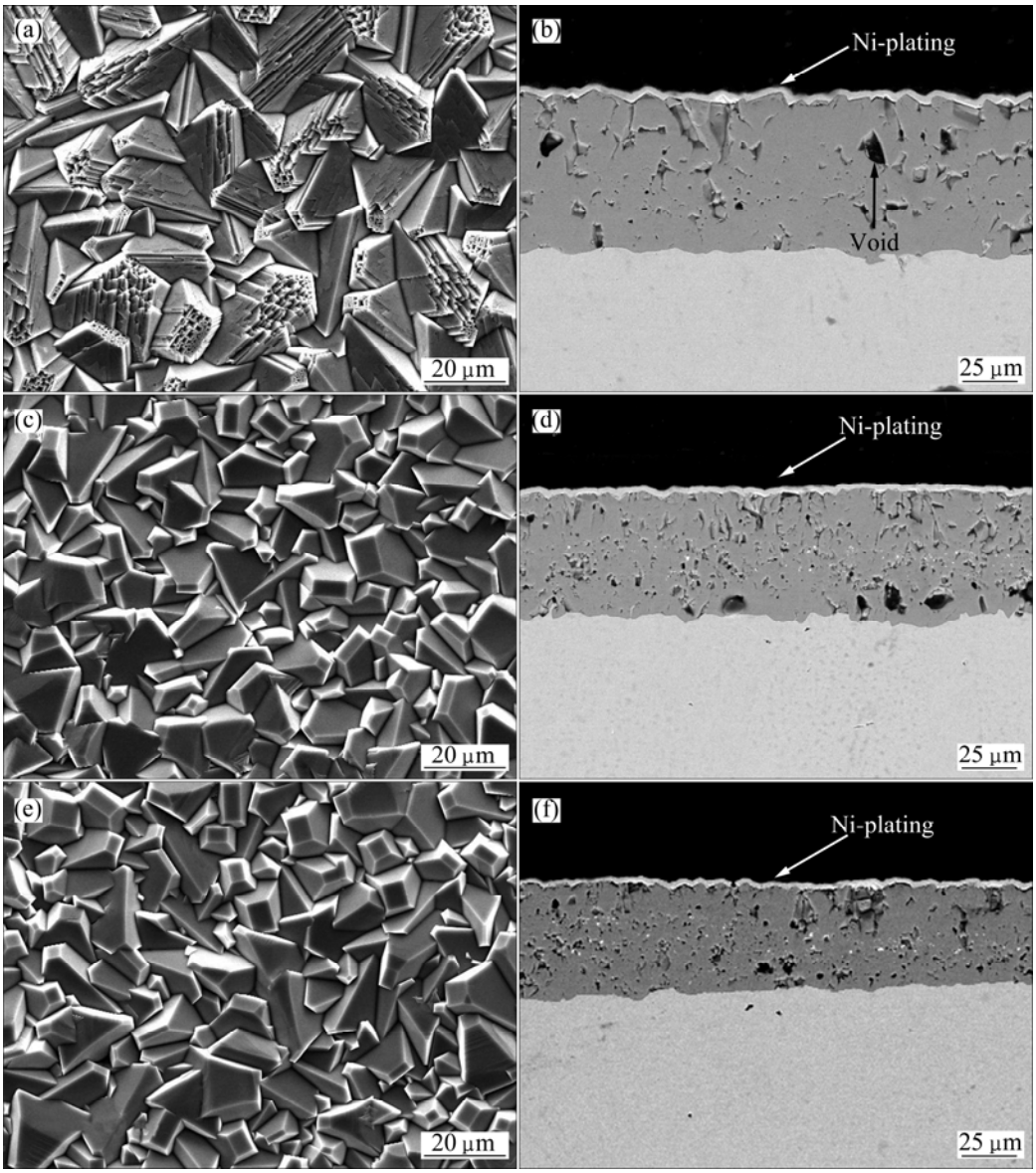

Fig. 8 Surface (a, c, e) and cross-sectional (b, d, f) morphologies of NiO scale formed on various samples after isothermal oxidation in air at 1150 °C for 20 h: (a), (b) Ni-film; (c), (d) Ni−1.2% CeO_2 nanocomposite coating; (e), (f) Ni−3.0% CeO_2 nanocomposite coating

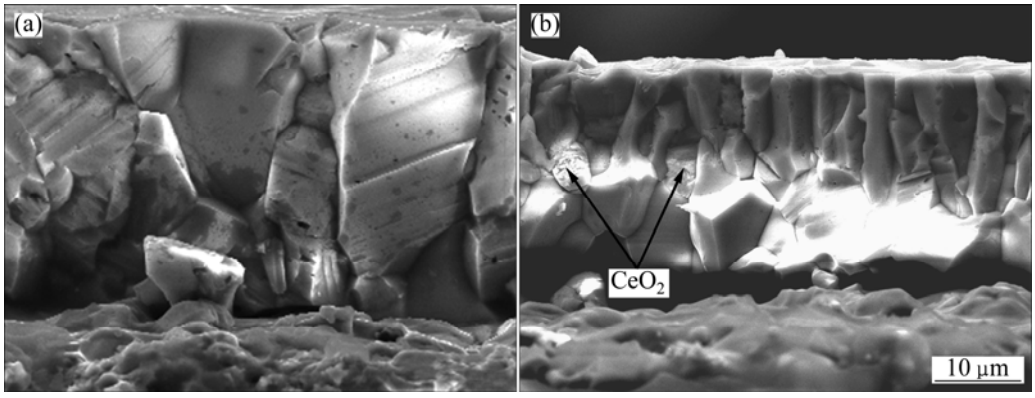

Fig. 9 Fracture sections of scales formed on Ni-film (a) and Ni−3.0% CeO_2 nanocomposite coating (b) after isothermal oxidation in air at 1050 °C for 20 h

faster than that on the electrodeposited pure Ni film due to an increase in the number of grain boundaries per unit volume in the scale [27,28]. However, the fact of a significant scaling rate reduction occurred. Although the scales formed on both films exhibited a similar duplex scale structure at 800 °C, the scales on the Ni−CeO_2 nanocomposite coatings exhibited a thicker inner layer, suggesting the predominantly inward oxygen diffusion over outer Ni diffusion. At temperatures above 1000 °C, the growth of Ni scale on the electrodeposited pure Ni film is dominantly outward-volume diffusion of nickel through NiO scales, which causes the formation of a simplex coarse columnar scale. However, for Ni−CeO_2 nanocomposite coatings, a duplex scale with similar thickness occurred, implying a similar diffusion rate between inward oxygen and outward Ni. The above results suggest that the addition of CeO_2 nanoparticles blocks the outer Ni diffusion along grain boundary to some extent and changes the oxidation growth mechanism from dominant outward Ni diffusion in the absence of RE into dominant inward oxygen diffusion at temperatures below 1000 °C.

At the onset of oxidation below 1000 °C, NiO nucleates, on the nanocrystalline Ni and CeO_2 nanoparticles; NiO scale grows rapidly and engulfs the CeO_2 nanoparticles on the surface. So, a continuous external coarse grain NiO scales without CeO_2 nanoparticles are developed by the healing of the NiO nuclei through their lateral growth during transient oxidation. After the transient stage of oxidation, an oxygen potential gradient is established in the metal-scale-gas system and the RE addition begins to take effect on the scale according to “dynamic-segregation theory” proposed by PINT [14]. RE ions from the added RE or its oxides by dissolution first segregate to metal/scale interface and then to the gas/scale interface through the scale-grain boundaries. When the concentration of RE ions at the scale grain boundaries reaches a critical value, the segregation-diffusion of RE ions blocks the outward diffusion of Ni and results in scale growth controlled primarily by inward diffusion of oxygen. However, experimental evidence for the assumption has been still lacking. PENG et al [8−10] found that the predominant outward diffusion of Ni along NiO grain boundaries was inhibited effectively by the segregated La ions at the grain boundaries originating from the added La_2O_3 nanoparticles by solution for Ni−La_2O_3 composite, which led to a reduction of the scaling rate and the formation of fine equiaxed crystal structure. HAUGSRUD [17] also found that the addition of sol−gel coatings of ceria particles below 20 nm onto a nickel surface retarded oxidation by blocking grain-boundary diffusion by segregated cerium ions. As a consequence, the inward oxygen diffusion controlled the growth of NiO for Ni−CeO_2 nanocomposite coatings. Since CeO_2 is relatively immobile and can be regard as inert remarks compared with Ni, the columnar outer layer/fine equiaxed inner layer interfaces correspond approximately to the original Ni−CeO_2 nanocomposite coating surface. With the oxidation progress, more CeO_2 particles incorporated into NiO oxide due to their inward growth may also dissolve, producing Ce ions segregated to the oxide grain boundaries and thus preventing the reduction of Ce concentration at the grain boundaries during a long oxidation time. At the same time, pinning [29] and “solute–drag” effect [14] of the dispersion particles at oxide grain boundaries gives rise to the formation of fine oxide grains, which provides indirect but credible evidence that the segregated Ce ions at the grain boundaries occurred and the outward diffusion of Ni was hindered to same extent by segregated Ce ions. This may be the reason that the oxide grains close to metal are finer than those near the scale surface. From Fig. 4 and Table 1, it could be also found that there was no much difference between the oxidation of Ni−CeO_2 nanocomposite coatings with different CeO_2 contents, especially at 1050 °C and 1150 °C, implying that the 0.8% CeO_2 particles can supply enough Ce ions segregated to grain boundaries of NiO to block the outward diffusion of Ni. From the above analysis, it can be found that the addition of CeO_2 particles in the Ni film blocks the outward diffusion of nickel and changes the oxidation growth mechanism, which causes a reduction of scaling rate because the inward oxygen diffusion is several orders of magnitude lower than the outward Ni diffusion at temperatures below 1000 °C. However, at temperatures above 1000 °C, the grain boundary diffusion of Ni should be neglected due to the outward-volume diffusion of Ni through NiO scales becoming the dominant−oxidation−growth mechanism [15−17, 25−28], thus the effect of CeO_2 particles and their content on decreasing the scaling rate through blocking the outward diffusion of Ni along grain boundaries decreased with the increasing oxidation temperature.

5 Conclusions

1) The CeO_2 nanoparticles co-electrodeposited successfully with Ni nanocrystalline to form the Ni−CeO_2 nanocomposite coatings.

2) The content of CeO_2 nanoparticles in the Ni−CeO_2 nanocomposite coatings increases with the increasing concentration of CeO_2 in the plating baths.

3) Compared with the electrodeposited pure Ni film, Ni−CeO_2 nanocomposite coatings showed a significant reduction in the isothermal oxidation rate at 800 °C due to the rapid outward diffusion of Ni along the grain boundaries inhibited by the second-phase CeO_2 particles and also by segregated Ce ions from the dissolution of CeO_2 nanoparticles which originally existed in the Ni−CeO_2 nanocomposite coatings.

4) The grain boundary diffusion of Ni could be neglected due to the outward-volume diffusion of Ni controlling the oxidation growth mechanism at 1050 °C and 1150 °C, thus the effect of CeO_2 particles and their content on decreasing the scaling rate decreased with the increasing oxidation temperature.

References

[1] TUSHAR B, SANDIP P H. Effect of electrodeposition conditions and reinforcement content on microstructure and tribological properties of nickel composite coatings [J]. Surf Coat Technol, 2011, 205: 4124−4134.

[2] ARUNA S T, WILLIAN GRIPS V K, RAJAM K S. Ni-based electrodeposited composite coating exhibiting improved microhardness, corrosion and wearresistance properties [J]. Journal of Alloys and Compounds, 2009, 468: 546−552.

[3] LEKKA M, ZANELLA C, KLORIKOWSKA A, BONORA P L. Scaling-up of the electrodeposition process of nano-composite coating for corrosion and wear protection [J]. Electrochim Acta, 2010, 55: 7876−7883.

[4] XUE Yu-jun, JIA Xian-zhao, ZHOU Yan-wei, MA Wei, LI Ji-shun. Tribological performance of Ni−CeO_2 composite coatings by electrodeposition [J]. Surf Coat Technol, 2006, 200: 5677−5681.

[5] SEN R, DSA S, DAS K. Effect of stirring rate on the microstructure and microhardness of Ni−CeO_2 nanocomposite coating and investigation of the corrosion property [J]. Surf Coat Technol, 2011, 205: 3847−3855.

[6] XUE Yu-jun, LI Ji-shun, MA Wei, ZHOU Yan-wei, DUAN Ming-de. Sliding wear behaviors of electrodeposited nickel composite coatings containing micrometer and nanometer La_2O_3 particles [J]. Journal Materials Science, 2006, 41: 1781−1784.

[7] TIAN Liang-liang, XU Jin-cheng. Electrodeposition and characterization of Ni−Y_2O_3 composite [J]. Appl Surf Sci, 2011, 257: 7615−7620.

[8] PENG X, PING D H, LI T F, WU W T. Oxidation behaviour of a Ni−La_2O_3 codeposited film on nickel [J]. J Electrochem Soc, 1995, 145: 389−398.

[9] PENG X, LI T, WU W. Effect of La_2O_3 particles on the oxidation of electrodeposited nickel films [J]. Oxid Met, 1999, 51: 291−315.

[10] PENG X, LI T, WU W, PAN W P. Effect of La_2O_3 particles on microstructure and cracking-resistance of NiO scale on electrodeposited nickel films [J]. Mater Sci Eng A, 2001, 298: 100−109.

[11] PFEIL L B. Improvement in heat-resisting alloys: UK Patent, 459848[P]. 1937.

[12] MOON D P. Role of reactive elements in alloy protection [J]. Mater Sci Tech, 1989, 5: 754−763.

[13] MOON D P. The reactive element effect on the growth rate of nickel oxide scales at high temperature [J]. Oxid Met, 1989, 32: 47−66.

[14] PINT B A. Experimental observations in support of the dynamic segregation theory to explain the reactive-element effect [J]. Oxid Met, 1996, 45: 1−37.

[15] CZERWINSKI F, SZPUNAR J A, SMELTZER W W. Steady-stage growth of NiO scales on ceria-coated polycrystalline nickel [J]. J Electrochem Soc, 1996, 143: 3000−3007.

[16] CZERWINSKI F, SZPUNAR J A. The nanocrystalline ceria sol−gel coatings for high temperature application [J]. J Sol–Gel Sci Technol, 1997, 9: 103−114.

[17] HAUGSRUD R. On the influence of sol–gel derived CeO_2 coatings on high-temperature oxidation of Co, Ni and Cu [J]. Corros Sci, 2002, 44: 1569−1582.

[18] SEN R, DAS S, DAS K. Effect of stirring rate on the microstructure and microhardness of Ni−CeO_2 nanocomposite coating and investigation of the corrosion property [J]. Surf Coat Technol, 2011, 205: 3847−3855.

[19] QU N S, ZHU D, CHAN K C. Fabrication of Ni−CeO_2 nanocomposite by electrodeposition [J]. Scripta Mater, 2006, 54: 1421−1425.

[20] XU Yu-jun, LIU Hong-bin, LAN Ming-ming, LI Ji-shun, LI Hang. Effect of different electrodeposition methods on oxidation resistance of Ni−CeO_2 nanocomposite coating [J]. Surf Coat Technol, 2010, 204: 3539−3545.

[21] ZHOU Y B, HU H T, ZHANG H J. Oxidation behavior of aluminide coatings on carbon steel with and without electrodeposited Ni−CeO_2 film by low-temperature pack cementation [J]. Vacuum, 2011, 86: 210−217.

[22] GUGLIELMI N. Kinetics of the deposition of inert particles from electrolytic baths [J]. J Electrochem Soc, 1972, 119: 1009−1012.

[23] ZHOU Y B, QIAN B Y, ZHANG H J. Al particles size effect on the microstructure of the co-deposited Ni−Al composite coatings [J]. Thin Solid Films, 2009, 517: 3287−3291.

[24] ZHOU Y B, CHEN H, ZHANG H, WANG Y. Preparation and oxidation of an Y_2O_3-dispersed chromizing coating by pack-cementation at 800 °C [J]. Vacuum, 2008, 82: 748−753.

[25] PERALDI R, MONCEAU D, PIERAGGI B. Correlations between growth kinetics and microstructure for scales formed by high-temperature oxidation of pure nickel. I. Morphologies and microstructures [J]. Oxid Met, 2002, 58: 249−273.

[26] PERALDI R, MONCEAU D, PIERAGGI B. Correlations between growth kinetics and microstructure for scales formed by high-temperature oxidation of pure nickel. II. Growth kinetics [J]. Oxid Met, 2002, 58: 275−295.

[27] ATKONSON H V, TAYLOR R I, GOODE P D. Transport processes in the oxidation of Ni studied using tracers in growing NiO scales [J]. Oxid Met, 1979, 13: 519−543.

[28] ATKONSON H V. Evolution of grain structure in nickel oxide scales [J]. Oxid Met, 1987, 28: 353−389.

[29] HINDAM H M, WHITTLE D. Peg formation by short-circuit diffusion in Al_2O_3 scales containing oxide dispersions [J]. J Electrochem Soc, 1982, 129: 1147−1149.

Ni−CeO_2 纳米复合镀层的制备与氧化性能

张海军，周月波，孙俭峰

黑龙江科技学院 材料科学与工程学院，哈尔滨 150027

摘 要：向普通电镀液中加入不同含量平均颗粒尺寸为 7 nm 的 CeO_2 颗粒，在 Ni 表面复合电镀不同 CeO_2 颗粒含量的 Ni−CeO_2 纳米复合镀层。研究表明，CeO_2 纳米颗粒弥散分布在 10~30 nm 的 Ni 中。为了了解温度和 CeO_2 颗粒含量对 Ni−CeO_2 纳米复合镀层氧化性能的影响规律，对两种不同 CeO_2 颗粒含量的 Ni−CeO_2 纳米复合镀层和普通 Ni 镀层进行不同温度下的恒温氧化对比实验。氧化实验结果表明：在 800 °C 时，CeO_2 抑制了 Ni 沿晶界外扩散，从而明显增强了 Ni−CeO_2 纳米复合镀层的氧化性能；然而，在 1050 °C 和 1150 °C 时，由于 Ni 向外的体扩散控制 Ni 的氧化过程，此时 CeO_2 对提高 Ni−CeO_2 纳米复合镀层的氧化性能作用轻微；此外，CeO_2 颗粒含量对 Ni−CeO_2 纳米复合镀层的氧化性能无明显影响。

关键词：复合电镀；纳米涂层；氧化；活性元素效应

(Edited by Hua YANG)